ARTICLE

Photocatalytic and Conductive MWCNT/TiO_2 Nanocomposite Thin Films

Kwadwo E. Tettey,[†] Michael Q. Yee,[‡] and Daeyeon Lee*[,†]

Department of Chemical and Biomolecular Engineering and Department of Bioengineering, University of Pennsylvania, Philadelphia, Pennsylvania 19104

ABSTRACT A conductive and photocatalytic nanocomposite thin film comprising multiwalled carbon nanotubes (MWCNTs) and TiO_2 nanoparticles is fabricated based on layer-by-layer (LbL) assembly in a nonpolar solvent, toluene. An amphiphilic surfactant, aerosol OT (AOT), is used to impart opposite surface charge onto MWCNTs and TiO_2 in toluene. Our fabrication technique enables the incorporation of unoxidized MWCNTs into the nanocomposite thin films, and at the same time, provides a versatile method of fabricating conformal thin films over a large area. The physicochemical properties of MWCNT/TiO_2 nanocomposite thin films, including composition and photocatalytic activity, can be varied by changing the concentration of AOT during assembly. The electrical properties of the nanocomposite film, specifically its sheet resistance and conductivity, can also be tuned through changing the assembly conditions. In addition, we demonstrate that the incorporation of MWCNTs within our films leads to a significant enhancement of the photocatalytic activity of TiO_2. The conductivity and enhanced photocatalytic activity of MWCNT/TiO_2 thin films make them promising for the generation of highly efficient dye-sensitized solar cells (DSSCs).

KEYWORDS: titanium dioxide • carbon nanotubes • thin films • CNT/TiO_2 composites • photocatalysis

INTRODUCTION

Photocatalytic materials convert solar energy to chemical energy, making them useful for the decontamination of organics (1, 2) and biological pathogens (3, 4). Titanium dioxide (TiO_2) is one of several semiconductors with desirable photocatalytic properties which generates electron−hole pairs upon activation by ultraviolet (UV) light. These electron−hole pairs, in turn, create active species such as surface-associated OH radicals, photogenerated OH radicals, and superoxides ($O_2 \cdot$), which participate in subsequent chemical reactions leading to the degradation of organic contaminants (5).

The utility of TiO_2 as a photocatalyst, however, is often limited by the recombination of photogenerated electron−hole pairs (5). Suppression of electron−hole recombination is thought to be imperative for improving the photocatalytic activity of TiO_2 (5). One proposed method of achieving this task is by creating nanocomposites of TiO_2 and carbon nanotubes (CNTs). The unique characteristics of CNTs, such as their electron-accepting capability and conductivity, make them ideal for sequestering photogenerated electrons (6). These properties of CNTs could hinder electron−hole recombination, thus leading to the enhancement of TiO_2 photocatalytic activity. In addition, the suppression of electron−hole recombination in TiO_2 has been utilized to improve the efficiency of dye-sensitized solar cells (7) and photoelectrochemical solar cells (8).

CNT−TiO_2 nanocomposites have been prepared through a number of different techniques. These include hydrothermal treatment (7, 9), sol−gel coating of CNTs (10, 11), hydrolysis (12), electrodeposition (13), and electrospinning (14). A major drawback to many of these methods is that they typically depend on the oxidation of CNTs to prepare CNT/TiO_2 nanocomposites. Although the fabrication process can be readily facilitated using oxidation, such treatment typically involves the use of highly corrosive chemicals and drastically changes the electronic properties of CNTs by disrupting their conjugated structure. Such changes, in turn, degrade the efficacy of CNTs as electron acceptors and carriers (15, 16). In addition, the aforementioned methods of fabricating CNT/TiO_2 nanocomposites have been mostly used for the generation of bulk nanocomposites and do not provide a straightforward method for creating conformal thin films and coatings with precisely controlled composition and properties. The generation of CNT/TiO_2 thin films would enhance the utility of these nanocomposites in various applications.

One versatile method of fabricating nanocomposite thin films is layer-by-layer (LbL) assembly, which involves sequential deposition of oppositely charged species on a substrate (17). Previous reports have demonstrated that photocatalytic thin films composed of TiO_2 nanoparticles and charged polymers can be generated by LbL assembly (18−22). Incorporation of CNTs into TiO_2 thin films using LbL assembly could further enhance their photocatalytic activity. However, LbL nanocomposite thin films composed of CNTs have been generally prepared using oxidized CNTs paired with an oppositely charged polymer in aqueous solutions (23−25). Although high temperature hydrogen treatment can be used to reduce the oxidized bonds in CNTs, the complete recovery of the pristine properties of CNTs is

* Corresponding author. E-mail: daeyeon@seas.upenn.edu.
Received for review May 27, 2010 and accepted August 9, 2010
[†] Department of Chemical and Biomolecular Engineering, University of Pennsylvania
[‡] Department of Bioengineering, University of Pennsylvania
DOI: 10.1021/am1004656

Published on Web 08/19/2010

difficult (26). While unoxidized CNTs have been incorporated into LbL films from aqueous solutions using anionic surfactants (27), aromatic surfactants (28, 29) and copolymers (30), such approaches typically require the utilization of newly synthesized molecules for the stabilization of CNTs.

In this report, we demonstrate that conductive and photocatalytic MWCNT/TiO_2 nanocomposite thin films can be generated based on LbL assembly. We fabricate LbL thin films comprising unoxidized MWCNTs and TiO_2 nanoparticles in a novel fashion. This is achieved by imparting surface charge onto MWCNTs and TiO_2 in a nonpolar medium, followed by the LbL assembly of each charged species. Our LbL approach enables the incorporation of unoxidized MWCNTs into thin films without the need for their oxidation through harsh chemical treatments. The objective of this paper is to demonstrate that the growth behavior and electrical properties of MWCNT/TiO_2 thin films can be controlled by varying the assembly parameters, and that the presence of MWCNTs enhances the photocatalytic activity of TiO_2 nanoparticles.

EXPERIMENTAL SECTION

Electrophoretic Mobility Measurements. MWCNT and TiO_2 particle suspensions in toluene containing AOT (AOT/toluene) were made by first preparing 0.1 wt % of particles in pure toluene (Fisher). 200, 100, 20, 10, 2, and 1 mM AOT (Sigma-Aldrich) in toluene were also prepared in separate vials. The 0.1 wt % TiO_2 powder (Degussa P25) and MWCNTs (Cheap Tubes Inc.) in pure toluene was sonicated for 1 h then mixed with an equal volume (3 mL) of AOT/toluene solutions to obtain 0.05 wt % particles in 100, 50, 10, 5, 1, and 0.5 mM AOT/toluene. Particle suspensions in AOT/toluene were sonicated for an additional hour. TiO_2 suspensions were allowed to sediment overnight and MWCNTs were filtered through a 5 μm PTFE filter before being used for electrophoretic mobility measurements. Electrophoretic mobility measurements were made with a Beckman Coulter Delsa NanoC at a field voltage of 85.2 V/cm.

Layer-by-Layer Assembly of MWCNTs and TiO_2. AOT/toluene solutions (60 mL) were prepared by making a 400 mM AOT stock solution followed by dilution to 200, 100, 20, and 10 mM solutions. TiO_2 (0.1 wt %) and MWCNTs (60 mL) were prepared in pure toluene and sonicated for 1 h. An equal volume (30 mL) of AOT/toluene solutions and 0.1 wt % particle suspension in pure toluene were mixed together and sonicated for 1 h to yield 0.05 wt % TiO_2 and MWCNTs in 200, 100, 50, 10, and 5 mM AOT/toluene. LbL assembly of MWCNTs and TiO_2 was performed on glass slides (Fisherbrand) cleaned by sonication in NaOH (1 M) for 20 min followed by rinsing in deionized (D.I.) water (18.2 MΩ cm) and drying with compressed air. The cleaned glass slides were exposed to the prepared solutions in the following order: 0.05 wt % MWCNTs in AOT/toluene, AOT/toluene rinse, toluene, and toluene followed by 0.05 wt % TiO_2 in AOT/toluene, AOT/toluene rinse, toluene, and toluene. The concentration of AOT in the AOT/toluene rinse baths was kept at the same concentration as in particle suspensions. A StratoSequencer VI (NanoStrata Inc.) was programmed to expose slides in particle suspensions for 10 min, followed by 2, 1, and 1 min in rinse baths.

MWCNT/TiO_2 Film Characterization. Absorbance measurements on films were made using a Cary 5000 (Varian Inc.) UV-Vis-NIR spectrophotometer. The absorbance at 500 nm was used for all data analysis. SEM images were taken with an FEI 600 Quanta FEG ESEM at 5 kV. Sheet resistance measurements were taken with a four-point probe station comprising a Cascade Microtech C4S 4-Point probe head, HP power supply unit and Keithley 2000 multimeters. Voltage and current measurements were taken at 10 random locations on each MWCNT/TiO_2 film. These values were subsequently used to calculate the sheet resistance. Thickness measurements were made with a Zygo NewView 6K series optical profilometer. To get an averaged film thickness, height profiles along a line segment were integrated and normalized with the length of the profile. Film thickness and sheet resistance measurements were used to calculate film conductivities. TGA measurements were taken with a TA Instruments SDT Q600. Samples for TGA were prepared by scraping off 60-bilayer films into a platinum TGA pan. The temperature was ramped from room temperature to 110 at 10 °C/min then held for 20 min to remove residual moisture. Following this, the temperature was increased to 1000 °C at a ramp rate of 10 °C/min and in air. Surface coverage was determined by analyzing SEM images using image analysis software ImageJ. The image threshold was adjusted until all MWCNT/TiO_2 domains were covered. From this, the surface coverage was calculated as the ratio between the area of MWCNT/TiO_2 domains and the total image area.

Photocatalytic Activity of MWCNT/TiO_2 Films. Photocatalysis experiments were performed by using 5 mg/L Procion Red MX-50 dye (Sigma-Aldrich) in D.I. water as the model organic contaminant. The glass slides on which MWCNT/TiO_2 films were prepared were cut to make use of only the regions with assembled films. For consistency, the same film areas were used for each set of experiments. The slides were placed in a plastic Petri dish containing dye solution (7 mL). The Petri dish was covered with a quartz slide to minimize evaporation. A UV lamp (UVP Inc.) was placed 6.7 cm above the Petri dish followed by insulation of the setup from external light. Longwave UV (365 nm, 6 W) was used for all experiments. 500 μL of dye sample was collected every 30 min for UV−vis analysis. For this analysis, the absorbance at the peak (538 nm) was monitored to determine the concentration change of the dye solution. Single component TiO_2 films were formed by calcining MWCNT/TiO_2 films at 600 °C for 1 h. The same procedure described above was used to probe the photocatalytic activity of single component TiO_2 films. X-ray diffraction (XRD) analysis was performed using a Rigaku GeigerFlex D/Max-B powder diffractometer equipped with a Cu Kα source. The fate of AOT after photocatalysis was probed by using FTIR spectroscopy. 30-bilayer MWCNT/TiO_2 films from 100 mM AOT suspensions were deposited on two CaF_2 FTIR windows (Thorlabs Inc.). Each sample was placed in a plastic Petri dish containing D.I. water. While the first film was kept in the dark for 5 h, the second was irradiated with 365 nm UV for the same period. A Nicolet 8700 FTIR spectrometer (Thermo Scientific) was used for data acquisition.

RESULTS AND DISCUSSION

Charging of MWCNT and TiO_2 in Toluene. Particles in nonpolar solvents tend to be colloidally unstable when no electrostatic or steric repulsion exists between them (31). To suspend multiwalled carbon nanotubes (MWCNTs) and TiO_2 nanoparticles by electrostatic repulsion in a low permittivity solvent, toluene ($\varepsilon = 2.3$), a charge inducing agent, aerosol OT (AOT), was used. In nonpolar solvents, it is believed that AOT molecules form reverse micelles, a small fraction of which undergo spontaneous disproportionation to from oppositely charged micelles (32, 33). Although TiO_2 and MWCNTs could not be dispersed in pure toluene, TiO_2 became well dispersed throughout our AOT concentration range (0.5−100 mM) and MWCNTs became well-dispersed in solutions with AOT concentration

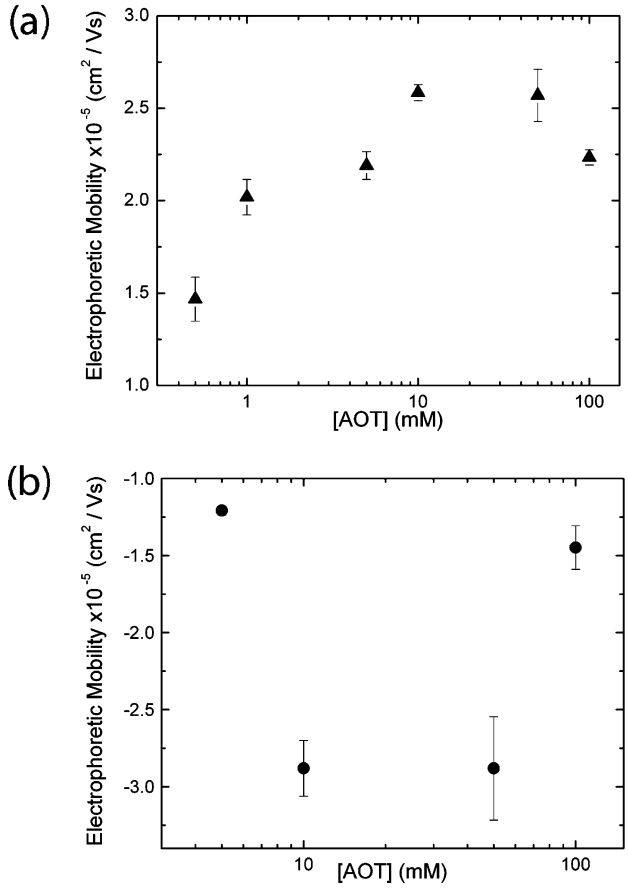

FIGURE 1. Electrophoretic mobility of dispersed (a) TiO_2 and (b) MWCNTs as a function of [AOT] present in toluene solution. Error bars represent standard deviations of three measurements. TiO_2 nanoparticles acquire a positive charge, whereas MWCNTs become negatively charged in AOT/toluene.

of 5 mM and greater (see Figure S1a,b in the Supporting Information).

To observe the change in surface charge of TiO_2 and MWCNTs in toluene with varying concentrations of AOT ([AOT]), electrophoretic mobility measurements were taken as shown in panels a and b in Figure 1, respectively. The electrophoretic mobility of both TiO_2 and MWCNTs is seen to depend on [AOT]. Interestingly, TiO_2 particles acquired positive charge, whereas MWCNTs became negatively charged in AOT/toluene solutions. Our recent study also showed that while a carbon-based material (carbon black) became negatively charged, an oxide (alumina) became positively charged in AOT/toluene solutions (34). Although the exact mechanism of particle charging via AOT is not clearly understood (33, 35), it has been proposed that the different charging behavior of particles can be attributed to the difference in their surface polarity (36) or to the difference in the relative acidity of the surfactant and functional groups on the particle surface (37, 38). Panels a and b in Figure 1 show that the magnitude of the electrophoretic mobility of TiO_2 and MWCNTs increases with [AOT] and have maximum magnitude between 10−50 mM AOT. We believe that, as the concentration of AOT increases beyond a peak value, AOT counterions overcrowd and screen the surface leading to a decrease in the surface charge (39). To

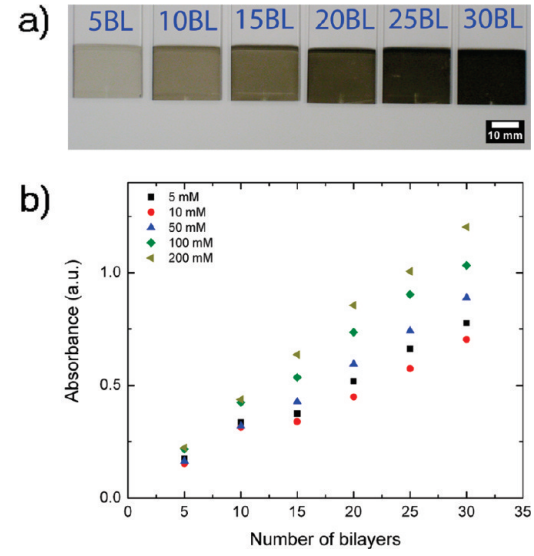

FIGURE 2. (a) Picture of MWCNT/TiO_2 films assembled on glass slides with 50 mM AOT in MWCNT and TiO_2 solutions. The blue text on glass slide represents the number of bilayers (e.g., 5BL = 5 bilayers). (b) Absorbance (measured at 500 nm) of MWCNT/TiO_2 films on glass slides as a function of the number of bilayers. Absorbance measurements were taken for 5 mM ■, 10 mM •, 50 mM ▲, 100 mM ♦, and 200 mM (left-facing triangle) MWCNT/TiO_2 films.

the best of our knowledge, this is the first report on stabilizing unoxidized CNTs in a nonpolar medium based on electrostatic repulsion. This new approach will be useful for processing CNTs for the generation of nanocomposites as well as for studying the solution properties of electrostatically stabilized CNTs (40, 41).

Layer-by-Layer (LbL) Deposition of Charged MWCNT and TiO_2 in Toluene. LbL assembly of MWCNTs and TiO_2 suspended in a wide range of AOT concentration was performed on glass slides to generate MWCNT/TiO_2 nanocomposite thin films. These nanocomposite films became darker with increasing number of deposited bilayers as shown in Figure 2a. UV−vis absorbance measurements (Figure 2b) also show that the absorbance of the films increases with the number of bilayers. The increase in absorbance as a function of deposited bilayers is linear for each assembly condition, indicating that the incorporation of MWCNTs within the film is linear. Such linear growth is often observed for LbL assembly of oppositely charged materials in aqueous solutions (42). The slope of the absorbance as a function of deposited bilayers is also seen to vary with the concentration of AOT in solution. This dependence indicates that changing the concentration of AOT is a convenient method of controlling film growth and composition during LbL assembly in nonpolar media, a direct analogy to controlling the pH and/or ionic strength of aqueous solutions (17).

The morphology of MWCNT/TiO_2 nanocomposite films was investigated using scanning electron microscopy (Figure 3). These images reveal that the surface coverage of MWCNT/TiO_2 films increases with the number of deposited bilayers. For 5- and 10-bilayer films (Figure 3a,b), MWCNT and TiO_2 particles are seen to cluster into isolated domains on the surface. These isolated clusters of TiO_2 and MWCNTs con-

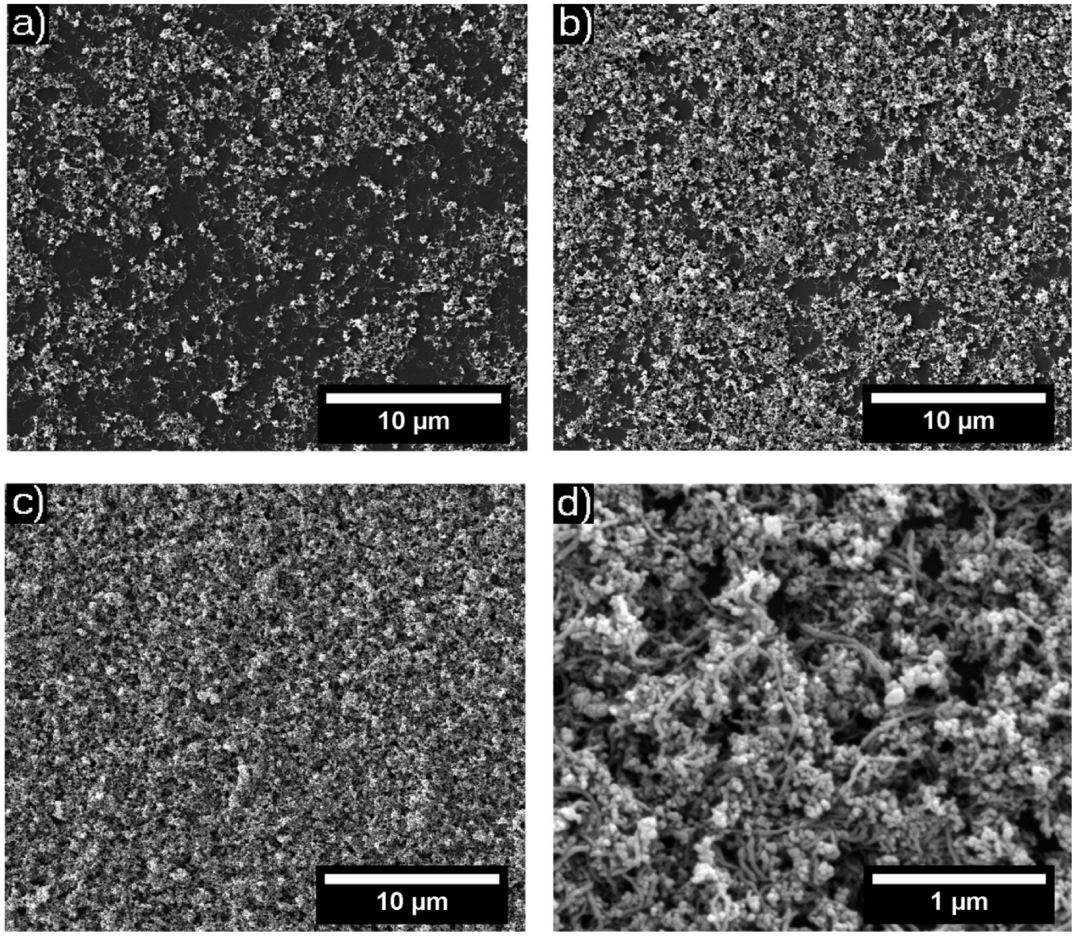

FIGURE 3. SEM images comparing the morphology of MWCNT/TiO_2 films for (a) 5, (b) 10, and (c, d) 30 bilayers. MWCNT/TiO_2 films were generated using particles suspended in 50 mM AOT/toluene solutions.

tinue to grow laterally until, a contiguous film is formed as seen in Figure 3c. Because the Debye length of charged species in AOT/toluene solutions is very large due to the low dielectric constant of the solution (43), the long-range electrostatic repulsion between particles with the same charge likely plays a significant role in the formation of particle domains on the surface. Similar transitions in film morphology have been observed for LbL assembly of oppositely charged nanomaterials in aqueous media (17) as well as in our recent study of LbL assembly of oppositely charged carbon black and alumina in toluene (34).

Images c and d in Figure 3 illustrate the porous nature of our MWCNT/TiO_2 films. High film porosities are particularly advantageous for catalysis applications. Previous studies based on the LbL assembly of oppositely charged nanoparticles have also shown that porous structures are useful for controlling the wetting and optical properties of surfaces (44, 45). A high magnification image of a 30-bilayer film (Figure 3d) shows that MWCNTs are homogeneously dispersed in the film, maximizing the contact area between MWCNTs and TiO_2. Homogeneous dispersion of MWCNTs within the film is important for forming a continuous network for electron transport and for preventing the recombination of photogenerated electron–hole pairs.

Film Composition. UV–vis absorbance measurements show that the absorbance of our nanocomposite films depends on [AOT], suggesting that the composition of the films is changing. To confirm this observation, the mass fractions of AOT, MWCNTs, and TiO_2 in films assembled from solutions with varying [AOT] were quantified by using thermogravimetric analysis (TGA). The composition of films obtained from TGA thermograms are summarized in Table 1. The results show that the [AOT] affects the composition of films fabricated from different assembly conditions. The increase in mass fraction of MWCNTs due to changing assembly conditions, albeit small, suggests that the [AOT] can be used to tune film composition.

Table 1. Composition of MWCNT/TiO_2 Films Assembled with Different [AOT]

[AOT] (mM)	AOT (%)	MWCNT (%)	TiO_2 (%)
50	6.0	12.1	81.9
100	7.4	13.1	79.5
200	7.5	13.8	78.7

Conductivity of MWCNT/TiO_2 Films. CNT/TiO_2 nanocomposites have shown great promise for their application in photocatalysis and photovoltaics. This is primarily because the conjugated structure of CNTs enables them to act as excellent carriers through which electrons can transport efficiently. This property is especially attractive for generating working electrodes for dye-sensitized solar cells (DSSCs) because the continuous pathway for electron trans-

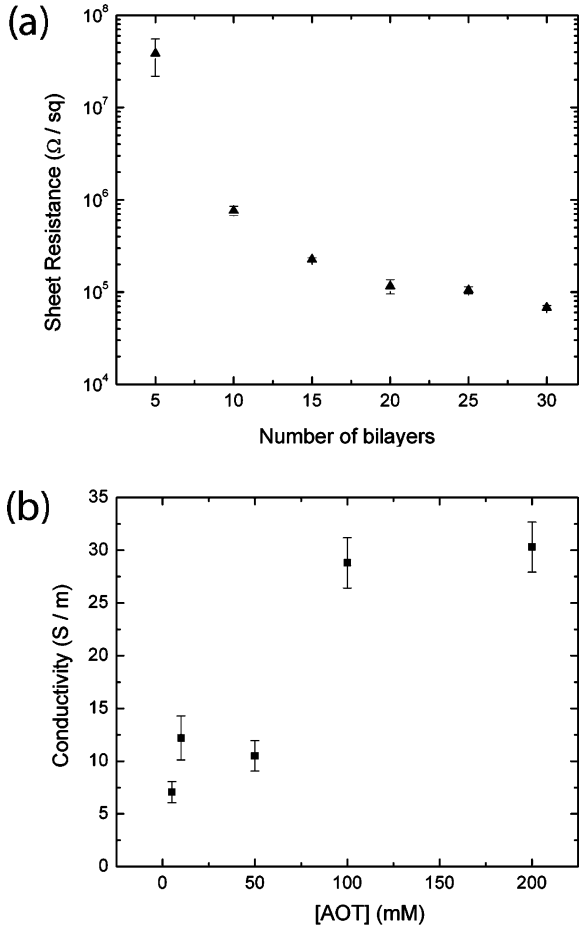

FIGURE 4. (a) Sheet resistance measurements as a function of number of desposited bilyaers for MWCNT/TiO_2 films fabricated from 200 mM AOT suspensions. (b) Conductivity of 30-bilayer MWCNT/TiO_2 films as a function of [AOT]. Error bars indicate standard deviations for 10 measurements.

port ensures an efficient collection of photogenerated electrons produced by TiO_2 nanoparticles (7). In addition to this application, conductive films could have useful roles for applications such as capacitors and batteries (46, 47).

We studied the effect of MWCNTs on the conductivity of our nanocomposite films by taking sheet resistance measurements as a function of the number of deposited bilayers as shown in Figure 4. The observed decrease in sheet resistance (Figure 4a) with increasing number of deposited bilayers indicates that the MWCNT/TiO_2 films become more conductive. We attribute this increase in conductivity to an increase in MWCNTs in the films and, more importantly, to the increased percolation of MWCNTs within the nanocomposite film as more bilayers are deposited. As the isolated domains of TiO_2 and MWCNTs on the substrate begin to merge, they form contiguous films as seen in morphological transitions in Figure 3.

The results from thermogravimetric analysis (TGA) of the MWCNT/TiO_2 composite films (Table 1) show that AOT is incorporated within the nanocomposite films during LbL assembly. It is likely that AOT forms thin layers on MWCNTs and TiO_2, which could influence the conductivity of the nanocomposite thin film. Although AOT is an insulator, the nanocomposite films are, nevertheless, conductive. Other

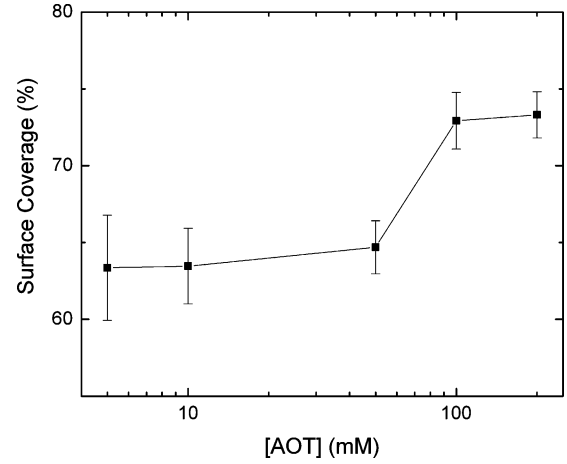

FIGURE 5. Surface coverage of 20-bilayer MWCNT/TiO_2 films as a function of concentration of AOT.

studies that generate LbL composite films containing CNTs have shown that the films are conductive despite the presence of insulating organic materials (27). It also has been reported that the conductivity in nanocomposites does not necessarily require uninterrupted electrical contact between MWCNTs, but rather needs sporadic ohmic connections between MWCNTs (30). Electron transport from TiO_2 to MWCNTs could occur based on a similar mechanism. Interestingly, our attempts to selectively remove AOT via thermal treatment at 400 °C under inert conditions led to a negligible change in the conductivity of MWCNT/TiO_2 nanocomposite thin films.

The effect of assembly conditions (i.e., the concentration of AOT) on the conductivity of MWCNT/TiO_2 films is illustrated by conductivity values for 30-bilayer films as shown in Figure 4b. Here, the conductivity of the LbL films increases with the [AOT]. We believe the observed trend is a result of an increase in MWCNT loading in the films as the [AOT] is increased. This hypothesis is supported by the fact that as the concentration of AOT is increased, UV–vis and TGA measurements show a corresponding increase in MWCNTs within the film.

Figure 4b also shows that the conductivity of 30-bilayer MWCNT/TiO_2 films lies in two distinct groups. The conductivity of 5, 10, and 50 mM samples are comparable, but smaller than 100 and 200 mM samples. The higher conductivity of 100 and 200 mM films is ascribed to the dense network of MWCNTs within these films. SEM images of 20-bilayer MWCNT/TiO_2 nanocomposite films assembled at different AOT concentrations highlight the differences in film morphology for a fixed number of bilayers. While films assembled with 5, 10, and 50 mM AOT solutions are seen to have nonuniform surface coverage (Figure S2a–c in the Supporting Information), those generated in 100 and 200 mM AOT solutions form a homogeneous network of MWCNT/TiO_2 nanocomposite (see Figure S2d,e in the Supporting Information). The surface coverage of 20-bilayer films, quantified as seen in Figure 5, confirms that the surface coverage of films indeed lie in two distinct groups. 100 mM and 200 mM samples are seen to have comparable surface coverage, which are larger than the surface coverage of 5,

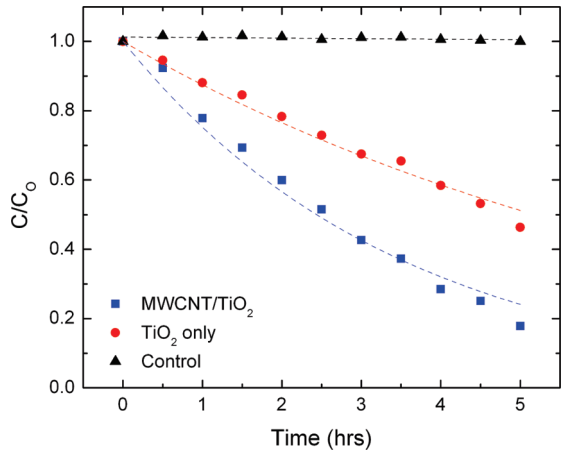

FIGURE 6. Comparison of photocatalytic activity for 30-bilayer 50 mM TiO_2 films with and without MWCNTs. Control sample contains no film.

10, and 50 mM samples. This result clearly indicates that by changing the assembly condition, it is possible to control the physical properties of MWCNT/TiO_2 nanocomposite thin films.

Enhanced Photocatalytic Activity of MWCNT/TiO_2 Films. As previously mentioned, the excellent electron accepting properties of CNTs could aid in suppressing the recombination of photogenerated electron−hole pairs. Furthermore, CNTs within nanocomposites increase the specific area available for adsorption of pollutants (6). As a result of these effects, CNT/TiO_2 nanocomposite structures are expected to have enhanced photocatalytic activity compared to single-component TiO_2 structures (6). We study the enhancement effect of MWCNTs by comparing the photocatalytic activity of 30-bilayer TiO_2 thin films assembled from 50 mM AOT suspension with and without MWCNTs. Single-component TiO_2 thin films were prepared by removing MWCNTs from the MWCNT/TiO_2 nanocomposite films through high temperature calcination at 600 °C for 1 h. The characterization of calcined films using UV−vis spectroscopy and scanning electron microscopy showed that MWCNTs were completely removed (see Figures S3 and S4 in the Supporting Information). In addition, the calcination of TiO_2 nanoparticles at 600 °C for 1 h showed little influence on the crystal structure and size of TiO_2 nanoparticles (see Figure S5 in the Supporting Information for X-ray diffraction of TiO_2). By removing MWCNTs via calcination, we can directly assess the effect of MWCNTs on the photocatalytic activity of TiO_2 nanoparticle thin films (48).

The decomposition of a model contaminant (an organic dye, Porcion Red) by MWCNT/TiO_2 nanocomposite thin films under UV irradiation was monitored using UV−vis spectroscopy. The photodegradation results shown in Figure 6 clearly show that the incorporation of unoxidized MWCNTs enhances the photocatalytic activity of TiO_2 nanoparticle thin films. The kinetic analysis of dye decomposition under UV irradiation using a Langmuir−Hinshelwood model (49) indicates that the incorporation of MWCNTs leads to an approximately 2-fold increase in the pseudofirst order rate constant. It is possible that the residual AOT could adversely influence the photocatalytic activity of as-assembled MWCNT/TiO_2 films. Selective removal of AOT via thermal treatment at 400 °C under N_2, however, led to a slight decrease in the rate constant compared to as-assembled MWCNT/TiO_2 films. This result could be due to a small loss of MWCNTs during the thermal treatment. We note that residual AOT in MWCNT/TiO_2 films undergoes degradation during photocatalysis as evidenced by Fourier transform infrared spectroscopy (FTIR) results (see Figure S6 in the Supporting Information).

Table 2. Rate Constants of Photocatalytic Reactions Using 25-Bilayer MWCNT/TiO_2 Films Assembled with Different [AOT]

[AOT] (mM)	k (h^{-1})
5	0.42
50	0.52
100	0.53
200	0.58

The effect of assembly conditions on the photocatalytic activity of MWCNT/TiO_2 nanocomposite thin films was also investigated. The photocatalytic rate constants for 25-bilayer MWCNT/TiO_2 nanocomposite thin films fabricated at different assembly conditions are summarized in Table 2. The results show that, in general, the photocatalytic activity of the nanocomposite films increases with [AOT], which indicates that a positive correlation exists between the composition, conductivity and photocatalytic activity of these nanocomposite thin films. Our results again illustrate that the properties of MWCNT/TiO_2 nanocomposite thin films assembled in nonpolar media can be tuned by varying the assembly condition (i.e., the concentration of AOT).

CONCLUSION AND OUTLOOK

In conclusion, we have demonstrated that conductive and photocatalytic MWCNT/TiO_2 nanocomposite thin films can be created by using LbL assembly in a nonpolar solvent. LbL assembly in toluene was achieved in a novel way by using a charge-inducing agent, AOT, to impart a negative surface charge on MWCNTs and a positive surface charge on TiO_2. Although our experimental results suggest that electrostatic interactions could play a key role in the adsorption of MWCNTs and TiO_2 during LbL, the relative significance of electrostatic interactions compared to other attractive forces such as van der Waals and depletion interactions (50) has not been established yet; this aspect warrants further study (51).

One advantage of our new approach in the generation of MWCNT/TiO_2 nanocomposites is that oxidation of MWCNTs is not necessary, thus preserving the efficacy of MWCNTs as an electron transporter. The incorporation of MWCNTs in these thin films significantly enhanced the photocatalytic activity of TiO_2 while the physicochemical properties of MWCNT/TiO_2 could also be varied by controlling the assembly condition. In addition to decontamination of water, MWCNT/TiO_2 nanocomposite thin films have great potential for the photolysis of water for hydrogen generation (52). Work is presently underway to fabricate dye-sensitized solar cells (8) using our LbL approach in nonpolar solvents.

Acknowledgment. This work was partly supported by the PENN MRSEC DMR-0520020 and the Nano/Bio Interface Center through the National Science Foundation NSEC DMR-0425780. We thank Professors Russell Composto and Cherie Kagan (University of Pennsylvania) for the use of their UV−vis spectrophotometers, Professor Chris Murray (University of Pennsylvania) for use of the FTIR spectrometer, and Professor Robert Carpick (University of Pennsylvania) for the use of the optical profilometer. We also thank Prof. Jason Baxter and Hasti Majidi (Drexel University) for their help with the use of solar illuminator for photocatalysis experiments and Rainer Küngas (University of Pennsylvania) for assistance with XRD measurements. We thank Evonik-Degussa for their generous provision of TiO_2—P25 and Beckman Coulter for their assistance with zeta-potential measurements.

Supporting Information Available: Photographs of TiO_2 and MWCNT particle suspensions in AOT/toluene, SEM images of 20-bilayer films fabricated from different assembly conditions, SEM images and UV−vis spectra for MWCNT/TiO_2 films and TiO_2 only films, XRD patterns for untreated and calcined TiO_2—P25, FTIR spectra for MWCNT/TiO_2 films before and after UV treatment (PDF). This material is available free of charge via the Internet at http://pubs.acs.org.

REFERENCES AND NOTES

(1) Heller, A. *Acc. Chem. Res.* **1995**, *28*, 503–508.
(2) Hoffmann, M. R.; Martin, S. T.; Choi, W. Y.; Bahnemann, D. W. *Chem. Rev.* **1995**, *95*, 69–96.
(3) Ireland, J. C.; Klostermann, P.; Rice, E. W.; Clark, R. M. *Appl. Environ. Microbiol.* **1993**, *59*, 1668–1670.
(4) Sunada, K.; Kikuchi, Y.; Hashimoto, K.; Fujishima, A. *Environ. Sci. Technol.* **1998**, *32*, 726–728.
(5) Fox, M. A.; Dulay, M. T. *Chem. Rev.* **1993**, *93*, 341–357.
(6) Woan, K.; Pyrgiotakis, G.; Sigmund, W. *Adv. Mater.* **2009**, *21*, 2233–2239.
(7) Muduli, S.; Lee, W.; Dhas, V.; Mujawar, S.; Dubey, M.; Vijayamohanan, K.; Han, S. H.; Ogale, S. *ACS Appl. Mater. Interfaces* **2009**, *1*, 2030–2035.
(8) Kongkanand, A.; Dominguez, R. M.; Kamat, P. V. *Nano Lett.* **2007**, *7*, 676–680.
(9) Byrappa, K.; Dayananda, A. S.; Sajan, C. P.; Basavalingu, B.; Shayan, M. B.; Soga, K.; Yoshimura, M. *J. Mater. Sci.* **2008**, *43*, 2348–2355.
(10) Luo, Y. S.; Liu, J. P.; Xia, X. H.; Li, X. Q.; Fang, T.; Li, S. Q.; Ren, Q. F.; Li, J. L.; Jia, Z. *Mater. Lett.* **2007**, *61*, 2467–2472.
(11) Wu, Y. C.; Liu, X. L.; Ye, M.; Xie, T.; Huang, X. M. *Acta Phys.-Chim. Sin.* **2008**, *24*, 97–102.
(12) Chen, L.; Zhang, B. L.; Qu, M. Z.; Yu, Z. L. *Powder Technol.* **2005**, *154*, 70–72.
(13) Jiang, L. C.; Zhang, W. D. *Electroanalysis* **2009**, *21*, 988–993.
(14) Aryal, S.; Kim, C. K.; Kim, K.-W.; Khil, M. S.; Kim, H. Y. *Mater. Sci. Eng., C* **2008**, *28*, 75–79.
(15) Hirsch, A. *Angew. Chem., Int. Ed.* **2002**, *41*, 1853–1859.
(16) Lee, S. W.; Kim, B. S.; Chen, S.; Shao-Horn, Y.; Hammond, P. T. *J. Am. Chem. Soc.* **2009**, *131*, 671–679.
(17) Decher, G.; Schlenoff, J. B. *Multilayer Thin Films: Sequential Assembly of Nanocomposite Materials* Wiley-VCH: Weinheim, Germany, 2003.
(18) Kim, T. H.; Sohn, B. H. *Appl. Surf. Sci.* **2002**, *201*, 109–114.
(19) Lvov, Y.; Ariga, K.; Onda, M.; Ichinose, I.; Kunitake, T. *Langmuir* **1997**, *13*, 6195–6203.
(20) Krogman, K. C.; Lowery, J. L.; Zacharia, N. S.; Rutledge, G. C.; Hammond, P. T. *Nat. Mater.* **2009**, *8*, 512–518.
(21) Lee, J. A.; Krogman, K. C.; Ma, M. L.; Hill, R. M.; Hammond, P. T.; Rutledge, G. C. *Adv. Mater.* **2009**, *21*, 1252–1256.
(22) Krogman, K. C.; Zacharia, N. S.; Grillo, D. M.; Hammond, P. T. *Chem. Mater.* **2008**, *20*, 1924–1930.
(23) Mamedov, A. A.; Kotov, N. A.; Prato, M.; Guldi, D. M.; Wicksted, J. P.; Hirsch, A. *Nat. Mater.* **2002**, *1*, 190–194.
(24) Rouse, J. H.; Lillehei, P. T. *Nano Lett.* **2003**, *3*, 59–62.
(25) Correa-Duarte, M. A.; Kosiorek, A.; Kandulski, W.; Giersig, M.; Liz-Marzan, L. M. *Chem. Mater.* **2005**, *17*, 3268–3272.
(26) Hamilton, C. E.; Lomeda, J. R.; Sun, Z.; Tour, J. M.; Barron, A. R. *Nano Lett.* **2009**, *9*, 3460–3462.
(27) Park, Y. T.; Ham, A. Y.; Grunlan, J. C. *J. Phys. Chem. C* **2010**, *114*, 6325–6333.
(28) Paloniemi, H.; Ääritalo, T.; Laiho, T.; Liuke, H.; Kocharova, N.; Haapakka, K.; Terzi, F.; Seeber, R.; Lukkari, J. *J. Phys. Chem. B* **2005**, *109*, 8634–8642.
(29) Paloniemi, H.; Lukkarinen, M.; Ääritalo, T.; Areva, S.; Leiro, J.; Heinonen, M.; Haapakka, K.; Lukkari, J. *Langmuir* **2005**, *22*, 74–83.
(30) Gheith, M. K.; Sinani, V. A.; Wicksted, J. P.; Matts, R. L.; Kotov, N. A. *Adv. Mater.* **2005**, *17*, 2663–2670.
(31) Hiemenz, P. C.; Rajagopalan, R., *Principles of Colloid and Surface Chemistry*, 3rd ed.; Marcel Dekker: New York, 1997.
(32) Roberts, G. S.; Sanchez, R.; Kemp, R.; Wood, T.; Bartlett, P. *Langmuir* **2008**, *24*, 6530–6541.
(33) Hsu, M. F.; Dufresne, E. R.; Weitz, D. A. *Langmuir* **2005**, *21*, 4881–4887.
(34) Tettey, K. E.; Yee, M. Q.; Lee, D. *Langmuir* **2010**, *26*, 9974–9980.
(35) Kemp, R.; Sanchez, R.; Mutch, K. J.; Bartlett, P. *Langmuir* **2010**, *26*, 6967–6976.
(36) Smith, P. G.; Patel, M. N.; Kim, J.; Milner, T. E.; Johnston, K. P. *J. Phys. Chem. C* **2007**, *111*, 840–848.
(37) Fowkes, F. M.; Jinnai, H.; Mostafa, M. A.; Anderson, F. W.; Moore, R. J. *ACS Symp. Ser.* **1982**, *200*, 307–324.
(38) Poovarodom, S.; Berg, J. C. *J. Colloid Interface Sci.* **2010**, *346*, 370–377.
(39) Keir, R. I.; Suparno; Thomas, J. C. *Langmuir* **2002**, *18*, 1463–1465.
(40) Davis, V. A.; Parra-Vasquez, A. N. G.; Green, M. J.; Rai, P. K.; Behabtu, N.; Prieto, V.; Booker, R. D.; Schmidt, J.; Kesselman, E.; Zhou, W.; Fan, H.; Adams, W. W.; Hauge, R. H.; Fischer, J. E.; Cohen, Y.; Talmon, Y.; Smalley, R. E.; Pasquali, M. *Nat. Nanotechnol.* **2009**, *4*, 830–834.
(41) Hough, L. A.; Islam, M. F.; Hammouda, B.; Yodh, A. G.; Heiney, P. A. *Nano Lett.* **2006**, *6*, 313–317.
(42) Decher, G.; Hong, J. D.; Schmitt, J. *Thin Solid Films* **1992**, *210*, 831–835.
(43) Sainis, S. K.; Merrill, J. W.; Dufresne, E. R. *Langmuir* **2008**, *24*, 13334–13347.
(44) Lee, D.; Rubner, M. F.; Cohen, R. E. *Nano Lett.* **2006**, *6*, 2305–2312.
(45) Lee, D.; Omolade, D.; Cohen, R. E.; Rubner, M. F. *Chem. Mater.* **2007**, *19*, 1427–1433.
(46) Frackowiak, E.; Beguin, F. *Carbon* **2001**, *39*, 937–950.
(47) Frackowiak, E.; Beguin, F. *Carbon* **2002**, *40*, 1775–1787.
(48) Although it would be desirable to compare the specific area of MWCNT/TiO_2 films to single-component TiO_2 films, MWCNT/TiO_2 LbL films with more than 4000 bilayers (impratically large number of bilayers) would be required to determine the specific surface area of these films using the BET method.
(49) Yu, Y.; Yu, J. C.; Yu, J. G.; Kwok, Y. C.; Che, Y. K.; Zhao, J. C.; Ding, L.; Ge, W. K.; Wong, P. K. *Appl. Catal., A* **2005**, *289*, 186–196.
(50) Asakura, S.; Oosawa, F. *J. Chem. Phys.* **1954**, *22*, 1255–1256.
(51) Bucur, C. B.; Sui, Z.; Schlenoff, J. B. *J. Am. Chem. Soc.* **2006**, *128*, 13690–13691.
(52) Park, J.; Choi, W. *J. Phys. Chem. C* **2009**, *113*, 20974–20979.

AM1004656